Evidence for Size-Dependent Discrete Dispersions in Single-Wall Nanotubes

A. Kasuya,[1] Y. Sasaki,[2] Y. Saito,[3] K. Tohji,[4] and Y. Nishina[1,2]
[1]*Institute for Materials Research, Tohoku University, Sendai 980-77, Japan*
[2]*Department of Basic Science, Ishinomaki Senshu University, Ishinomaki 986, Japan*
[3]*Department of Electrical and Electronic Engineering, Mie University, Tsu 514, Japan*
[4]*Department of Geoscience and Technology, Tohoku University, Sendai 980-77, Japan*
(Received 23 December 1996; revised manuscript received 18 February 1997)

Raman scattering spectra of single-wall nanotubes with mean radii 0.55, 0.65, and 1.0 nm show size-dependent multiple splittings of the optical phonon peak corresponding to the E_{2g} mode in graphite. These splittings constitute the first experimental evidence for the unique feature of nanotubes that they exhibit discrete and diameter-dependent dispersions arising from their cylindrical symmetry. The observed dispersion is well explained on the basis of graphite, and shows possibilities of predicting and controlling the basic property of nanotubes in the zone-folding scheme. [S0031-9007(97)03354-1]

PACS numbers: 61.46.+w

One of the most fundamental aspects of nanometer-scale materials is their size-dependent physical and chemical properties [1]. The carbon nanotube, of single-wall type [2–6] particularly, is an ideal substance to study because its simple structure is defined unambiguously by its diameter, length, and chirality, and its size-specific properties are analyzed on the basis of graphite. Theoretically [7–11], a nanotube is predicted to be an insulator or a metal depending on its diameter and chirality. The reason comes from the fact that the translational symmetry in a single layer of graphite remains along the tube axis but no longer exists around its circumference which turns to a cyclic one. Thus, the wave vectors of both electrons and phonons remain to take continuous values along the direction corresponding to the tube axis in the Brillouin zone, but can take only sets of discrete values around the circumference determined by its cyclic period. This size-dependent zone-folding effect is the salient feature of nanotube that governs its basic property, but has never been studied experimentally on single-wall tubes to date.

This Letter presents a direct experimental evidence on the size-specific discrete dispersion in the phonon system of single-wall nanotubes as determined by our Raman scattering measurements. In graphite, Raman scattering is allowed only for optical phonons of wave vector $q = 0$ because of the momentum conservation. In nanotubes, on the other hand, it is allowed [10] also for finite but discrete values of q's in the graphite Brillouin zone determined by the cyclic symmetry mentioned above. Our experimental results show that such phonons at discrete q's exhibit size-dependent multiple splittings of the Raman peak. From the analysis of splittings, the diameter-dependent dispersion relation has been determined for the first time in the phonon system of nanotube, and explained in terms of the graphite dispersion.

Single-wall monosize nanotubes were synthesized by an arc discharge method with the positive graphite electrode mixed with different metals such as Ni/Fe, Co, and La. Our electron microscopic observation shows that the mean radii of these samples prepared with Ni/Fe, Co, and La are 0.55, 0.65, and 1.0 nm, respectively. The radius distribution is measured under electron microscope and is rather sharp, and its half-width is less than 0.1 nm for each sample. Details of sample preparation process are given in our previous publications [6]. The samples are prepared and optimized in a great number of conditions to obtain maximum concentrations of single-wall tubes compared with other carbonaceous materials. Our carbon soot contains a high concentration of single-wall nanotubes in the deposit on the ceiling right above the carbon electrodes in the discharge chamber. The concentrations in selected samples are (20–30)% for Fe/Ni, more than 10% for Co, and 6% for La as estimated by visual inspections of our electron microscope images.

Figure 1 shows our Raman scattering spectra measured in a backscattering geometry with 514.5 nm line of Ar-ion laser. The top spectrum, 1(a), represents Raman scattering from nanotubes prepared by graphite electrodes with the positive side mixed with Ni and Fe (mean tube radius 0.55 nm), and 1(b) with Co (0.65 nm), and 1(c) with La (1.0 nm). Figure 1(d) is from multiwall tubes of 5 nm average radius deposited on the negative electrode of pure graphite, and 1(e) from crystalline graphite (highly oriented pyrolytic graphite). Comparing with 1(e), spectra 1(a), 1(b), and 1(c) show multiple splittings of the Raman peak centered at 1580 cm^{-1} of E_{2g} (stretching) mode in graphite. Figure 1(a) shows three well resolved peaks at 1590.9, 1567.5, and 1549.2 cm^{-1} indicated by arrows. Figure 1(b) shows two peaks at 1589.3 and 1569.8 cm^{-1} followed by a weak shoulder on the lower energy side initiated by a kink indicated by "⊣" mark, and 1(c) a peak at 1586.2 cm^{-1} followed by two shoulders. The spectral splittings represented by peaks and kinks are narrower in going from the spectrum 1(a) to 1(b) to 1(c). As the splittings decrease, peaks appear to turn to shoulders and then merge to the peak position of graphite, 1(e), shown in the bottom spectrum. These spectral features are quite reproducible in both intensity and spectral position

 0031-9007/97/78(23)/4434(4)$10.00

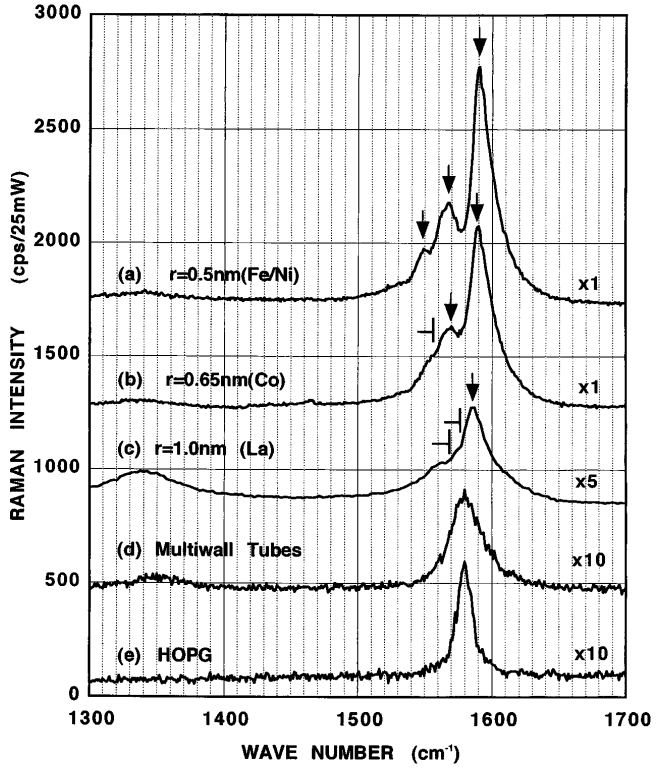

FIG. 1. Raman scattering spectra measured with Ar-ion laser at 514.5 nm line in the region from 1300 to 1700 cm^{-1} of single-wall nanotubes prepared with Ni/Fe (the top spectrum), Co (second), La (third), and of multiwall (fourth), and of highly oriented pyrolytic graphite (bottom). The positions of peaks are indicated by arrows and kinks by "⊣" marks.

as confirmed in our measurements made on a numerous number of samples and sample positions. Intensity ratios between peaks and kinks in each spectrum are reproducible over each species of samples within 15%. The peaks always appear at the spectral positions with the mean deviation of ± 0.5 cm^{-1}. Only spectral sharpness varies slightly from sample to sample, being more apparent for those exhibiting higher Raman intensities of the peaks. In sharper spectra, shoulders tend to form peaks. The positions of peaks and shoulders can be determined more accurately by some line-profile analysis, but not uniquely without further information such as line-shape functions.

The highly systematic and reproducible spectral features found in 1(a), 1(b), and 1(c) strongly indicate that the splitting comes from a physical mechanism inherent to nanotubes of different radius and not due to any extrinsic reason such as contributions from various carbonaceous materials in our samples. Spectral contributions from such materials must be very small because of the extremely low Raman intensity near 1350 cm^{-1} of our spectra. Extensive Raman measurements [12,13] show that any graphitic networks having finite (<100 nm) size or many defects exhibit rather broad and strong Raman peaks near 1350 cm^{-1} comparable to that in the vicinity of 1580 cm^{-1}. The spectrum 1(d) of multiwall tubes is broader and shows no definite structure or shift compared with 1(e) of graphite. Spectra in Fig. 1, therefore, show that our samples of nanotubes are rather long and defect free.

Raman measurements have been reported previously on single-wall nanotubes prepared with Co [14] as well as on multiwall tubes [15]. Neither of them, however, depicted the size-dependent multiple splittings. The former measurement [14] shows spectral features similar to Fig. 1(b) in Fig. 1 but are recognized only as a doublet obscured by the dominant broad peaks between 1350 and 1580 cm^{-1} contributed from other carbonaceous materials. Figure 1(d) is quite similar to that of a previously measured one on multiwall tubes [15].

The observed multiple splittings of Raman spectra may be interpreted in terms of the phonon dispersion relation of a single-layer graphite [10]. Because of the cylindrical symmetry, its Brillouin zone consists of a set of equally spaced lines separated by the inverse of its radius, $1/r$, along the circumference direction in the hexagonal Brillouin zone of a graphite layer. Optical phonons of discrete wave vectors $q_n = n/r$ $(n = 0, 1, 2, \ldots)$ along this direction can be excited with their energies given by the dispersion relation of a graphite layer at the same q_n's provided; the dispersion remains unchanged by rolling up the graphite sheet into a closed tube [10,11].

Figure 2 shows a plot of observed energy positions of multiply split peaks denoted by arrows in Fig. 1 with respect to $1/r$ for each sample. Also indicated are positions of kinks by "⊤" marks which may serve as references for the energy position of observed shoulders. Dashed lines in Fig. 1 are optical phonon dispersions of longitudinal (LO) and transverse (TO) modes in graphite calculated along the Γ-M [13,16]. The abscissa, $1/r$, corresponds to the phonon wave vector q for the curves with $n = 1$, and $q/2$ for the curves with $n = 2$. Observed peak positions coincide well with $n = 1$ or $n = 2$ dispersion curves, showing the evidence of size-dependent discrete dispersion substantiated by our high enough accuracy and reproducibility of our measurements and narrow enough size distribution of our samples. The peaks (indicated by arrows) for each spectrum may be assigned, in order from the highest energy, to LO phonons with $n = 1$, TO phonons with $n = 1$, and TO phonons with $n = 2$, respectively. Those peaks fitted on the $n = 1$ curves correspond to optical phonons of the fundamental vibrations with their wavelength equal to the circumference of the tube, and $n = 2$ the first harmonic vibrations with their wavelength equal to $1/2$ of the circumference. These peaks with $n = 1$ and $n = 2$ are assigned to the Raman active E_1 and E_2 modes, respectively, for general chiral tubes [2] represented by the symmetry group $C_{N/\Omega}$. Other E_n modes with $n > 2$ are Raman inactive [10] and may contribute to the tails of the multiply split peak. The peak width of multiwall tubes shown in Fig. 1 is explained by the superposition of peaks contributed from nested single-wall tubes of varying radii up to 5 nm of mean outer radius.

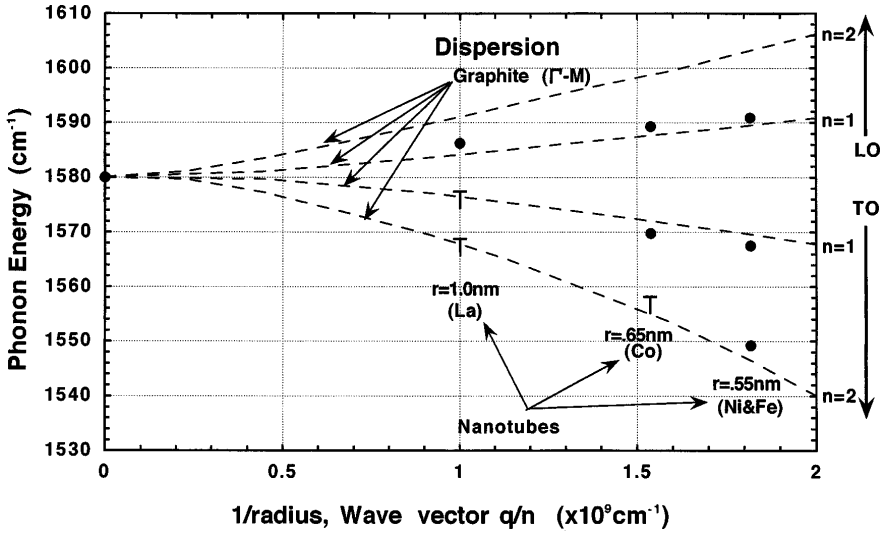

FIG. 2. Plot of observed energy positions of multiply split peaks denoted by arrows in Fig. 1 with respect to $1/r$ for nanotubes prepared with Fe/Ni ($r = 0.55$ nm), Co ($r = 0.65$ nm), and La ($r = 1.0$ nm). Dashed lines are theoretical LO and TO modes in graphite along the Γ-M [12,15]. The ordinate, $1/r$, corresponds to the phonon wave vector q for the curves with $n = 1$ (fundamental vibration), and wave vector $q/2$ with $n = 2$ (first harmonic vibration). The positions of kinks are indicated by "$\top$" marks as references for the position of shoulders.

The good agreement of experimental results with graphite dispersion shows that nanotubes with radii from 0.5 to 1.0 nm exhibit diameter-dependent discrete dispersion which is the unique feature not present in any other condensed matter existing. Our measurement constitutes the first spectroscopic proof that the sample consists of a closed hollow cylinder of a graphite single layer consisting of sp^2 bonded carbon networks. The diameter-dependent zone-folding effect arising from cylindrical symmetry is prominent and plays the essential role in understanding and predicting the basic properties of nanotubes in terms of graphite.

Raman spectral analysis gives definite and decisive information on the size and symmetry of nanotubes. The splittings of both Raman peaks and LO-TO modes displayed in Figs. 1 and 2 show that the diameter of nanotubes can be determined with an accuracy of less than 0.1 nm which is comparable to a hexagon distance (0.246 nm) along the circumference. The width of each split peak in Fig. 1 reflects the diameter distribution of our sample observed by our electron microscope.

The peak splitting depends also on the chirality of nanotubes, but the dependence is very small because LO-TO splittings do not depend much on the direction of q near Γ, being largest along Γ-M (armchair case, plotted in Fig. 2) and smallest along Γ-K (zigzag case, not shown but almost superposed on Γ-M) [13,16]. Hence, nanotubes having any chiral direction with the same diameter exhibit nearly equal peak splittings. The information on chirality is best obtained by examining the vibrational modes near M point which is folded onto Γ for armchair and zigzag tubes, and its vibrational modes become Raman active [10]. Figure 1 does not show strong peaks in the spectral range of the M-point modes between 1300 and 1500 cm^{-1}, indicating that our samples are chiral provided, Raman intensities of these allowed modes are not orders of magnitude smaller than those of LO and TO near Γ. Our electron diffraction study also indicates that our samples are chiral [3]. Detailed theoretical calculations of Raman intensity as well as frequency lead to further chirality analyses.

The experimental results in Fig. 1 show possible resonant effects that Raman intensities of optical phonons, particularly for LO modes, are an order of magnitude higher than that of graphite at $k = 0$. This, in fact, is the reason of high spectral contributions from nanotubes compared with other carbonaceous materials in our samples. Our preliminary measurement reveals that intensities of LO and TO vary notably with the wavelength of incident laser beam down to 800 nm, suggesting strong resonant couplings of the vibrational system with particular zone-folded electronic states of nanotube. The above intensity dependence is strongly diameter dependent. Our previous measurements [17] on nanotubes made with Fe/Ni show Raman peaks around 170 cm^{-1} corresponding to acoustic phonons. These peaks are also found to be strongly diameter dependent, and are shifted to around 160 cm^{-1} in nanotubes made with Co. Such strong diameter dependencies come from the fact that the acoustic phonon branch is much more sensitive to the wave vector (1/radius) than the optical one. These peaks also show strong resonant effects.

The rich and characteristic spectral features of nanotubes revealed newly in the present investigation as compared with graphite show that the Raman scattering may be the most specific and informative spectral tool to analyze nanometer-scale properties in terms of size and symmetry dependent vibrational and electronic states.

The authors would like to thank Professor C. Horie, Dr. M. Fukushima, and Dr. T. Maeda for valuable discussion. The work was supported in part by grant-in-aid for the New Program from the Ministry of Education, and CREST of Japan Science and Technology Corporation.

[1] See, for example, *Proceedings for the International Symposium on Small Particles and Inorganic Clusters*, edited by S. Sugano and Y. Nishina [Surf. Rev. Lett. **3** (1996)].
[2] S. Iijima and T. Ichihashi, Nature (London) **363**, 603 (1993).
[3] D. S. Bethune *et al.*, Nature (London) **363**, 605 (1993).
[4] Y. Saito *et al.*, Jpn. J. Appl. Phys. **33**, L526 (1994).
[5] A. Thess *et al.*, Science **273**, 483 (1996).
[6] Y. Saito, M. Okuda, and T. Koyama, Surf. Rev. Lett. **3**, 863 (1996).
[7] N. Hamada, S. Sawada, and A. Oshiyama, Phys. Rev. Lett. **68**, 1579 (1992).
[8] R. Saito, M. Fujita, G. Dresselhaus, and M. S. Dresselhaus, Appl. Phys. Lett. **60**, 2204 (1992).
[9] H. Ajiki and T. Ando, J. Phys. Soc. Jpn. **62**, 1255 (1993).
[10] R. A. Jishi, D. Inomata, K. Nakao, M. S. Dresselhaus, and G. Dresselhaus, J. Phys. Soc. Jpn. **63**, 2252 (1994).
[11] Jin Yu, Rajiv K. Kalia, and P. Vashista, J. Chem. Phys. **103**, 6697 (1995).
[12] F. Tuinstra and J. L. Koenig, J. Chem. Phys. **53**, 1126 (1970).
[13] M. S. Dresselhaus and G. Dresselhaus, *Light Scatterings in Solids III*, edited by M. Cardona and G. Guentherodt (Springer-Verlag, Berlin, 1982), Chap. 2.
[14] J. M. Holden *et al.*, Chem. Phys. Lett. **220**, 186 (1994).
[15] H. Hiura, T. W. Ebbesen, K. Takagi, and H. Takahashi, Chem. Phys. Lett. **202**, 509 (1993).
[16] M. Maeda, Y. Kuramoto, and C. Horie, J. Phys. Soc. Jpn. **47**, 337 (1979).
[17] A. Kasuya, Y. Saito, Y. Sasaki, M. Fukushima, T. Maeda, C. Horie, and Y. Nishina, *Science and Technology of Atomically Engineered Materials*, edited by P. Jena, S. N. Khanna, and B. K. Rao (World Scientific, Singapore, 1996), p. 431.